A THEORY OF JOVIAN SHADOW BURSTS

N. GOPALSWAMY
Indian Institute of Astrophysics, Kodaikanal, Tamil Nadu, India

(Received 29 March, 1985)

Abstract. The shadow events in the dynamic spectra of Jovian decametric emission are explained as the result of interaction between electron bunches responsible for S and L emissions. The relevant dispersion relation is derived for the fast extraordinary mode in the cold magnetospheric plasma in the presence of S and L electron bunches. The growth rate of the synchrotron maser instability is studied in the presence and absence of S-electrons. It is shown that the synchrotron maser instability responsible for L-emission can be temporarily quenched by the invasion of S-electrons, thereby stopping the L-emission. The theory accounts for various observed features of the shadow events.

1. Introduction

The Io-modulated ratio emission from Jupiter is classified into two types: (a) long time scale (L) bursts and (b) short time scale (S) bursts. Sometimes the two types of emissions occur simultaneously, and the dynamic spectrum of Jovian emission becomes complex. The most interesting phenomena during such S–L interaction is the so-called shadow events. The shadow events occur as tilted-V patterns in the dynamic spectra when the S-emission intersects the L-emission and, hence, also named as shadow-V bursts (SV's).

The S and L emissions are supposed to be due to independent mechanisms because of their spectral characteristics. It is generally accepted that relativistic electron beams streaming along the Io flux tubes are responsible for the Jovian decametric emissions. These electron beams could be generated by the magneto hydrodynamic waves induced by the motion of conducting Io in the Jovian magnetosphere (Gurnett and Goertz, 1981) and can generate both electrostatic and electromagnetic waves. The particular type of waves that will be predominantly generated depends upon the parameters of the magnetospheric plasma through which the beams propagate. In the Jovian magnetospheric plasma, the plasma frequency is much smaller than the electron cyclotron frequency, similar to the terrestrial case. Under such situations, cyclotron emission is more probable because the level of electrostatic turbulence excited by the electron beams will be very small to produce the observed electromagnetic radiation (Melrose, 1982). Since the magnetic field decrease from Jovian surface to the equatorial plane, the frequency of emission, occurring at local electron cyclotron frequency, should also decrease. This will result in a negative drift of the burst in the dynamic spectrum. If the electron beam moves towards the Jovian surface then one should get a positive drift. Since most of the S-bursts have negative drifts, the S-electron beams should propagate along the magnetic field lines away from the

Earth, Moon, and Planets **35** (1986) 93–115

Jovian surface. This conclusion must be in conformity with the polarisation. Observations show that the S-bursts are polarized in the right-hand sense at high frequencies and both types of polarisations occur when the frequency is below 20 MHz (Leblanc *et al.*, 1980). The polarisation in the left-hand sense led Galeev and Krasnoselskikh (1979) to conclude that Io emits relativistic particles to produce radiation in the O-mode so that one observed left-hand polarization. In this case, one should get only positive drift, contradicting observations because electron streams propagate towards the planet. Galeev and Krasnoselskikh (1979) failed to notice the fact that left-hand polarisation with negative drift can be obtained if the electron streams are injected from the planet from the southern hemisphere, because the electron streams propagate antiparallel to the magnetic field. Since the dipole of Jupiter is displaced and tilted, the maximum gyro frequency in the southern hemisphere is about 18 MHz. This explains the mixed polarisation below about 20 MHz and hence one need not assume that electrons are emitted by Io, as done by Galeev and Krasnoselskikh (1979). Another evidence for the fact that electrons are injected from the Jovian ionosphere is the increasing drift rates of S-bursts at high frequencies. If the stream goes towards the planet, then they will be reflected near the mirror points where the drift rate will be zero. In fact, it was demonstrated first by Desch *et al.* (1978) and confirmed by Leblanc *et al.* (1980) that the drift rate of S-bursts increase with frequency up to the highest frequency observed. It is clear from the above discussion that S-electrons must be injected into the Jovian magnetosphere from the planet.

The L-bursts, as a rule, show only slow frequency drifts, and the sign of the drift may vary erratically (Smith, 1976; Riihimaa and Carr, 1981). Probably, electrons causing these bursts are the ones reflected from both the mirror points of the magnetic field. Moreover, the L-emission is supposed to be due to a loss cone distribution of electrons produced by the loss of low pitch angle electrons in the stream into the ionosphere of the planet. In this case, of course, electrons could also be injected from Io which get mirrored, as discussed by Wu and Freund (1977). The point is, if one agrees with the existing model that L-emissions result from the synchrotron maser instability (SMI) in the X-mode, L-emission must be due to a loss cone distribution of electrons. It is immaterial whether the beam is injected into the Io flux tube (IFT) from the planet or from the satellite.

In the light of the above discussion, one has to explain the shadow events making use of the type of interference the S-electrons cause when they pass through the L-emission region. The cold magnetospheric plasma provides the base mode which is fed by the non-thermal electrons with a loss cone distribution. If an S-electron beam with a shifted Maxwellian distribution is added to the system consisting of the magnetospheric plasma and the L-electrons, then the loss cone responsible for L-emission is filled temporarily and hence the SMI is quenched, provided the S beam transit time through the L-emission region is sufficiently large compared to the growth time of the SMI. In this paper we will show that this is possible for the physical parameters relevant to the Jovian decametric emission.

The plan of the paper is as follows: In Section 2 we summarize the observations of shadow events and formulate the model in Section 3. The dispersion relation to the synchrotron maser instability in the presence of non-thermal beams is analysed in Section 4. The model is applied to the shadow events in Section 5, and finally, the conclusions are presented in Section 6.

2. Observational Characteristics of Shadow Events

The appearance of shadow bursts in the Jovian decametric emission was observed by several authors (e.g., Gordon, 1966; Riihimaa and Warwick, 1968; Ellis, 1973; Krausche *et al.*, 1976; Flagg *et al.*, 1976; Riihimaa *et al.*, 1981). These events were referred to as emission gaps (Riihimaa, 1977), absorption bursts (Ellis, 1973), fast drift shadow (FDS) events, tilted-V patterns, 'invisible bursts' (Riihimaa, 1981), and shadow-V bursts (Staelin and Rosenkranz, 1983). The shadow events were firmly established after the high time and spectral resolution observations of Riihimaa *et al.* (1981). The main characteristics of the shadow events can be summarized as follows.

2.1. Appearance

The shadow events occur as streaks of emission gaps across the L-emission. The dynamic spectra took like those of S-bursts excepting for the fact that they are in absorption. Most of the time, the shadow events are affiliated to the S-bursts. S-bursts are seen aligned along the edges of the emission gap, sometimes only on one edge. The S-bursts, in some cases, could be seen before and after the gap. It would appear that the two S-bursts originate from a common point, encounter an L-emission region where the L-emission in between the S-bursts is blocked and proceed beyond the L-emission region. Such V-shaped pairs of S-bursts have been observed and, probably, they occur only in this way most of the time (Groth and Dowden, 1975; Leblanc *et al.*, 1980; Riihimaa and Carr, 1981). At high frequencies, the shadow events occur in a very rapid succession. In such cases, the L-emission in between the shadow events are often confused with S-bursts. The affiliation of shadow events with S-bursts is clear from another fact that the highest frequency of the observed shadow events is the same as that of S-bursts (Riihimaa *et al.*, 1981). If the frequency of the L-emission is unstable, then the shadow events do not appear as clear tilted V-patterns and the whole dynamic spectrum may be quite complicated. In some cases, the S-bursts appear to grow out of the shadow bursts, the former being at lower frequencies.

2.2. Bandwidth

Since the shadow events occur only when there is an S–L intersection, their bandwidth is the same as that of L-bursts although they appear very clear when the L-emission bandwidth is large (> 0.5 MHz). If there are multiband L-emissions, and if there is a pair of S-bursts interacting with all the bands then again the L-emission between the two S-bursts in each band is cut-off.

2.3. Frequency drift

As mentioned already, the drift rates of the shadow events match precisely with the associated S-bursts. The drift rate $\dot{f}$ (MHz s^{-1}) is often of the order of the frequency of emission f (MHz). In cases where two S-bursts line up along the two boundaries of the shadow pattern, the drift rate of the shadow events is in between the drift rates of the affiliated S-bursts. The shadow events always drift negatively supporting the idea that the S-electrons are injected from the Jovian ionosphere.

2.4. Single frequency duration

At high frequencies where single streaks of shadow events are seen, the single frequency duration is almost the same as that of the S-bursts. At lower frequencies, the single frequency duration increases and lies in the range 10–100 ms. Also, the tilted V-pattern indicates that the S-burst aligned with the leading edge has slightly more drift rate than the trailing one. In terms of electron bunches causing the S-emission, the leading bunch travels faster than the trailing one and there are still some electrons in between the two bunches which probably cause the L-emission gap.

3. Possible Explanation of the Shadow Events

The possible interpretations of the shadow events could be classified into two broad categories. The first one is, the stoppage of L-emission in the generation stage itself. The second is the blocking of L-emission due to some agency in between the observer and the source. In the first case one has to find ways in which the process of L-emission generation can be stopped by the presence of S-emission. The problem essentially reduces to the question as to how the SMI is quenched during the time the S-electrons invade the L-emission region. In the second case the possible obstacles that can block or scatter the L-emission have to be identified such that the shadow events are produced. Apart from these, one can also envisage some kind of frequency swing of the L-burst emission. But then, it will not produce a tilted V-pattern and the S-burst affiliation cannot be accounted for. The idea that the S-electrons can block, scatter or refract the L-emission is probably not correct because of the very small density of the non-thermal beams. Even if there are some density inhomogeneities in the magnetospheric plasma traversed by the L-emitting beams, they cannot produce such regular drifting patterns. In the generation stage again, the parameters determining the SMI might change suddenly but it should be caused by the S-electrons. In view of these difficulties, the most probable mechanism seems to be the quenching of the SMI during the S-electron interference.

4. Theoretical Model

In accordance with the above discussions, we assume that the L and S emissions occur due to independent electron bunches. The cold magnetospheric plasma provides the

base mode, viz., the fast extraordinary mode which is fed by the L-electron bunch to directly generate the L-emission through SMI. The S-electron bunch or the group of electrons in between a pair of S-electron bunches enters the region of L-emission. The S-emission itself occurs due to the simple gyro-synchrotron mechanism whereby a part of the perpendicular energy of the S-bunch is converted into S-bursts (Staelin and Rosenkranz, 1983). We further assume that the S and L bunches do not disturb the dielectric properties of the cold magnetospheric plasma. Thus, we consider a three component plasma consisting of the cold magnetospheric plasma, the L-electron bunch and S-electron bunch, at the time of S–L interaction. We are interested in the stability of such a three component plasma for electromagnetic perturbations of the extraordinary type. We are concerned only with the linear theory and study of the linear growth rate in the presence and absence of an S-electron bunch. The non-linear theory will deal with the saturation of the SMI and related effects which will be useful to estimate the intensity of L-emission. We are only interested in showing that the L-emission will be stopped if the S-bunch can quench the SMI.

The maser type of instability was invokved by Hirshfild and Bekefi (1963) to explain the Jovian decametric emission, where the propagation was assumed to be perpendicular to the magnetic field. To explain the radiation in the fast X-mode, near the local electron frequency one has to assume oblique propagation. Such an attempt was made by Wu and Freund (1977) to explain Jovian decametric emission and Le Queau *et al.* (1984) to explain the auroral kilometric radiation with a loss cone beam. Full relativistic dispersion was considered by Pritchett (1984) with a delta function ring distribution and a relativistic generalization of the Dory–Guest–Harris distribution. Wu and Freund (1984) considered a hollow beam of electrons and showed that in the kinetic limit the hollow beam distribution is more unstable than the loss-cone distribution. Though there is extensive study of the SMI with various types of distributions (e.g., Melrose *et al.*, 1982; Hewitt *et al.*, 1982; Sharma *et al.*, 1982), we will consider only the case of loss cone type of distribution, because the final result is insensitive to the particular form of the distribution (Wu and Freund, 1977).

4.1. The dielectric tensor

Since the bandwidth of the SV's is small, we take the Jovian magnetic field to be locally straight along the z-coordinate of the cartesian system. The cold magnetospheric plasma dynamics is governed by the fluid equations. We neglect the ion dynamics in the magnetospheric plasma and consider only the dynamics of electron fluid. The dynamics of energetic particles is governed by the relativistic Vlasov equation. The electromagnetic fields are governed by Maxwell's equations. The electric and magnetic fields **E** and **B** and the displacement vector **D** of the perturbations are related by the Maxwell equations

$$\nabla \times \mathbf{E} = \frac{1}{c} \frac{\partial \mathbf{B}}{\partial t}, \tag{1}$$

$$\nabla \times \mathbf{B} = \frac{1}{c}\frac{\partial \mathbf{D}}{\partial t}, \tag{2}$$

$$\nabla \cdot \mathbf{D} = 0; \tag{3}$$

and the supplementary equation

$$\frac{\partial \mathbf{D}}{\partial t} = \frac{\partial \mathbf{E}}{\partial t} + 4\pi \mathbf{J}, \tag{4}$$

where $\mathbf{J}$ is the perturbed current density.

Eliminating $\mathbf{B}$ between Equations (1) and (2) one obtained the wave equation

$$\nabla \times (\nabla \times \mathbf{E}) + \frac{1}{c^2}\frac{\partial^2 \mathbf{D}}{\partial t^2} = 0. \tag{5}$$

The perturbed current is given by

$$\mathbf{J} = \mathbf{J}_c + \mathbf{J}_b, \tag{6}$$

which is the sum of the contributions due to the cold plasma $\mathbf{J}_c$ and that due to the energetic particles $\mathbf{J}_b$.

$\mathbf{J}_c$ can be obtained from the linearised fluid equation of motion

$$\frac{\partial \mathbf{V}}{\partial t} = -\frac{e}{m}\left(\mathbf{E} + \frac{\mathbf{V} \times \mathbf{B}_0}{c}\right), \tag{7}$$

where e and m are the charge and mass of the electron, $\mathbf{V}$ is the perturbed velocity of the electron fluid element, and c is the velocity of light. If we assume that each perturbed quantity x varies as

$$x \sim \exp(i\mathbf{k} \cdot \mathbf{r} - i\omega t), \tag{8}$$

where $\mathbf{k}$ and ω are the wave vector and frequency of the perturbation, Equation (7) becomes

$$i\omega \mathbf{V} = \frac{e}{m}\mathbf{E} + \mathbf{V} \times \boldsymbol{\omega}_c, \tag{9}$$

where $\boldsymbol{\omega}_c = e\mathbf{B}_0/mc$ is the vector electron cyclotron frequency, whose magnitude is given by

$$\omega_c = \frac{eB_0}{mc}.$$

Solving for $\mathbf{V}$ one gets

$$\mathbf{V} = \frac{e}{m(\omega_c^2 - \omega^2)}\left(\mathbf{E} - \boldsymbol{\omega}_c \times \mathbf{E} - i\frac{\boldsymbol{\omega}_c \cdot \mathbf{E}}{\omega}\boldsymbol{\omega}_c\right). \tag{10}$$

Therefore, the current density $\mathbf{J}_c$, given by

$$\mathbf{J}_c = -eN_c\mathbf{V} \tag{11}$$

where N_c is the unperturbed electron density of the magnetospheric plasma and can be written as

$$\mathbf{J}_c = -\frac{\omega_{pc}^2}{4\pi(\omega_c^2 - \omega^2)}\left[i\omega\mathbf{E} - \boldsymbol{\omega}_c \times \mathbf{E} - i\frac{\boldsymbol{\omega}_c \cdot \mathbf{E}}{\omega}\boldsymbol{\omega}_c\right], \tag{12}$$

where ω_{pc} is the cold plasma frequency.

The energetic electrons are described by the linearised relativistic Vlasov equation

$$\left[\frac{\partial}{\partial t} + \mathbf{v}\cdot\nabla - \frac{e}{m}\left(\mathbf{E} + \frac{\mathbf{v}\times\mathbf{B}}{c}\right)\cdot\frac{\partial}{\partial\mathbf{p}}\right] f_\alpha(\mathbf{r}, \mathbf{p}, t) =$$

$$= \frac{e}{m}\frac{\mathbf{v}\times\mathbf{B}_0}{c}\cdot\frac{\partial}{\partial\mathbf{p}} f_{0\alpha}(\mathbf{p}), \tag{13}$$

where $f_\alpha(\mathbf{r}, \mathbf{p}, t)$ and $f_{0\alpha}(\mathbf{p})$ are the perturbed and equilibrium distributions of the energetic electrons of type α. When we introduce the species index α, we have in mind the different distributions we are going to use for the S and L electron bunches. $\mathbf{p}$ and $\mathbf{v}$ are the relativistic particle momentum and velocity, related by

$$\mathbf{p} = m\gamma\mathbf{v}, \tag{14}$$

where

$$\gamma = (1 - v^2/c^2)^{-1} \tag{15}$$

is the relativistic factor. The perturbed current density $\mathbf{J}_b$ of the energetic particles is given by

$$\mathbf{J}_b = \sum_\alpha \int \mathrm{d}\mathbf{p}\, \mathbf{v} f_\alpha(\mathbf{r}, \mathbf{p}, t); \tag{16}$$

or, for perturbations of type (8),

$$\mathbf{J}_b(\mathbf{k}, \omega) = \sum_\alpha \int \mathrm{d}\mathbf{p}\, \mathbf{v} f_\alpha(\mathbf{k}, \mathbf{p}, \omega). \tag{17}$$

Equation (13) can be integrated by the usual method of characteristics (Baldwin *et al.*, 1969) to get f_α. Substituting for f_α in Equation (17) after a lengthy but straightforward algebra we find that

$$\mathbf{J}_b = \boldsymbol{\sigma}^b \cdot \mathbf{E}, \tag{18}$$

where

$$\boldsymbol{\sigma}^b = -\frac{i\omega}{4\pi}\sum_\alpha \frac{\omega_{p\alpha}^2}{\omega^2}\int_0^\infty 2\pi p_\perp \,\mathrm{d}p_\perp \int_{-\infty}^\infty \mathrm{d}p_\parallel \times$$

$$\times \sum_{q=-\infty}^{\infty} \frac{\gamma^{-1}\mathbf{T}_\alpha^q}{(\omega - k_\parallel v_\parallel - q\omega_c\gamma^{-1})}, \tag{19}$$

and

$$\mathbf{T}_\alpha^q = \begin{bmatrix} v_\perp U_\alpha \left(\frac{qJ_q}{\beta}\right)^2 & -iv_\perp U_\alpha \frac{J_q J_q'}{\beta} & v_\parallel W_\alpha^{(q)} \frac{J_q J_q'}{\beta} \\ iv_\perp U_\alpha \frac{J_q J_q'}{\beta} & v_\perp U_\alpha J_q J_q' & iv_\perp W_\alpha^{(q)} J_q J_q' \\ v_\parallel U_\alpha \frac{qJ_q^2}{\beta} & -iv_\parallel U_\alpha J_q J_q' & v_\parallel W_\alpha^{(q)} J_q^2 \end{bmatrix}, \tag{20}$$

$$U_\alpha = m\gamma\omega \frac{\partial f_{0\alpha}}{\partial p_\perp} + k_\parallel \left(p_\perp \frac{\partial f_{0\alpha}}{\partial p_\parallel} - p_\parallel \frac{\partial f_{0\alpha}}{\partial p_\perp}\right), \tag{21}$$

$$W_\alpha^{(q)} = m\gamma\omega \frac{\partial f_{0\alpha}}{\partial p_\parallel} - m \frac{q\omega_c}{p_\perp} \left(p_\perp \frac{\partial f_{0\alpha}}{\partial p_\parallel} - p_\parallel \frac{\partial f_{0\alpha}}{\partial p_\perp}\right). \tag{22}$$

In these expressions, $\parallel$ and $\perp$ refer to the components of vectors parallel and perpendicular to the equilibrium magnetic field $\mathbf{B}_0$. J_q and J_q' are the Bessel function of the first kind and its derivative, with argument $\beta = k_\perp v_\perp \gamma/\omega_c$; $\omega_{p\alpha} = (4\pi N_\alpha e^2/m)^{1/2}$ is the plasma frequency of the species α with density N_α. Now, γ is not very large compared to unity for a weakly relativistic plasma. Since we are considering fast extraordinary mode (X-mode) with frequency close to the local electron cyclotron frequency, the phase velocity of the perturbations is much larger than the velocity of light. Therefore, the argument of the Bessel functions $\beta \ll 1$, so that it is sufficient to keep $q = 0, \pm 1$ terms in Equation (19) – i.e.,

$$\begin{aligned} \boldsymbol{\sigma}^b = \frac{-i\omega}{4\pi} \sum_\alpha \frac{\omega_{p\alpha}^2}{\omega^2} \int_0^\infty 2\pi p_\perp \, \mathrm{d}p_\perp \int_{-\infty}^\infty \mathrm{d}p_\parallel \, \gamma^{-1} \times \\ \times \left\{ \frac{v_\parallel W_\alpha^{(0)}}{\omega - k_\parallel v_\parallel} \begin{bmatrix} 0 & 0 & 0 \\ 0 & 0 & 0 \\ 0 & 0 & 1 \end{bmatrix} + \right. \\ + \frac{v_\perp U_\alpha}{4(\omega - k_\parallel v_\parallel - \omega_c \gamma^{-1})} \begin{bmatrix} 1 & -i & 0 \\ i & 1 & 0 \\ 0 & 0 & 0 \end{bmatrix} + \\ \left. + \frac{v_\perp U_\alpha}{(\omega - k_\parallel v_\parallel + \omega_c \gamma^{-1})} \begin{bmatrix} 1 & i & 0 \\ -i & 1 & 0 \\ 0 & 0 & 0 \end{bmatrix} \right\}. \end{aligned} \tag{23}$$

Furthermore, since ω is close to ω_c and γ is slightly more than unity, the dominant contribution to the right-hand side of Equation (23) comes from the second term under the curly bracket. Therefore, one can write Equation (23) as

$$\boldsymbol{\sigma}^b = -\frac{i\omega}{4\pi}\frac{\varepsilon_b}{2}\begin{bmatrix} 1 & -i & 0 \\ i & 1 & 0 \\ 0 & 0 & 0 \end{bmatrix}, \tag{24}$$

where

$$\varepsilon_b = \sum_\alpha \frac{\omega_{p\alpha}^2}{\omega^2}\int_0^\infty 2\pi p_\perp \, \mathrm{d}p_\perp \int_{-\infty}^{\infty} \mathrm{d}p_\parallel \frac{\gamma^{-1} v_\perp U_\alpha}{(\omega - k_\parallel v_\parallel - \omega_c \gamma^{-1})}. \tag{25}$$

Now consider the Fourier transform of Equation (4) of the form

$$\mathbf{D}(\mathbf{k}, \omega) = \mathbf{E}(\mathbf{k}, \omega) + \frac{4\pi i}{\omega}\mathbf{J}(\mathbf{k}, \omega). \tag{26}$$

Substituting **J** from Equation (12) and (18) along with Equation (24) into (26), one gets

$$\mathbf{D}(\mathbf{k}, \omega) = \mathbf{E}(\mathbf{k}, \omega) + \frac{\omega_{pc}^2}{(\omega_c^2 - \omega^2)}\left[\mathbf{E}(\mathbf{k}, \omega) + \frac{i}{\omega}\boldsymbol{\omega}_c \times \mathbf{E}(\mathbf{k}, \omega) - \right.$$

$$\left. - \frac{1}{\omega^2}\boldsymbol{\omega}_c \cdot \mathbf{E}(\mathbf{k}, \omega) + \frac{\varepsilon_b}{2}\mathbf{R} \cdot \mathbf{E}(\mathbf{k}, \omega)\right], \tag{27}$$

where

$$\mathbf{R} = \begin{bmatrix} 1 & -i & 0 \\ i & 1 & 0 \\ 0 & 0 & 0 \end{bmatrix}. \tag{28}$$

Equation (28) can now be written in terms of the dielectric tensor $\boldsymbol{\varepsilon}$ as

$$\mathbf{D} = \boldsymbol{\varepsilon} \cdot \mathbf{E}, \tag{29}$$

where

$$\boldsymbol{\varepsilon} = \begin{bmatrix} \varepsilon_1 & -i\varepsilon_2 & 0 \\ i\varepsilon_2 & \varepsilon_1 & 0 \\ 0 & 0 & \varepsilon_0 \end{bmatrix} \tag{30}$$

and

$$\varepsilon_1 = 1 + \frac{\omega_{pc}^2}{\omega_c^2 - \omega^2} + \tfrac{1}{2}\varepsilon_b,$$

$$\varepsilon_2 = \frac{\omega_c}{\omega}\frac{\omega_{pc}^2}{\omega_c^2 - \omega^2} + \tfrac{1}{2}\varepsilon_b, \tag{31}$$

$$\varepsilon_0 = 1 - \frac{\omega_{pc}^2}{\omega^2}.$$

4.2. The dispersion relation

Since the X-mode is circularly polarised, it is convenient to work in the principal coordinate system in which the algebra becomes simpler. The transformation to the principal coordinate system (PCS) is defined by the following unitary transformation

$$\mathbf{E}' = \mathbf{U} \cdot \mathbf{E}, \tag{32}$$

where the prime denotes PCS. $\mathbf{U}$ is the unitary matrix defined by

$$\mathbf{U} = \frac{1}{\sqrt{2}} \begin{bmatrix} 1 & -i & 0 \\ 1 & i & 0 \\ 0 & 0 & \sqrt{2} \end{bmatrix} \tag{33}$$

with

$$\mathbf{U} \cdot \mathbf{U}^{\dagger} = \mathbf{U}^{\dagger} \cdot \mathbf{U} = \mathbf{I}, \tag{34}$$

where $\mathbf{U}^{\dagger}$ is the Hermitian adjoint of $\mathbf{U}$, given by

$$\mathbf{U}^{\dagger} = \frac{1}{\sqrt{2}} \begin{bmatrix} 1 & 1 & 0 \\ i & -i & 0 \\ 0 & 0 & \sqrt{2} \end{bmatrix} \tag{35}$$

and $\mathbf{I}$ is the unit tensor.

Now, the inverse transformation is

$$\mathbf{D} = \mathbf{U}^{\dagger} \cdot \mathbf{D}', \tag{36}$$

$$\mathbf{E} = \mathbf{U}^{\dagger} \cdot \mathbf{E}'. \tag{37}$$

Therefore, Equation (29) can be written as

$$\mathbf{U}^{\dagger} \cdot \mathbf{D}' = \boldsymbol{\varepsilon} \cdot \mathbf{U}^{\dagger} \cdot \mathbf{E}'. \tag{38}$$

Operating on Equation (38) from the left by $\mathbf{U}$ we get

$$\mathbf{D}' = \mathbf{U} \cdot \mathbf{E} \cdot (\mathbf{U}^{\dagger} \cdot \mathbf{E}'), \tag{39}$$

i.e.,

$$\mathbf{D}' = \boldsymbol{\varepsilon}' \cdot \mathbf{E}', \tag{40}$$

where

$$\boldsymbol{\varepsilon}' = \mathbf{U} \cdot \boldsymbol{\varepsilon} \cdot \mathbf{U}^{\dagger} \tag{41}$$

is the dielectric tensor in the PCS. Substituting for $\boldsymbol{\varepsilon}$ from Equation (30) one gets

$$\boldsymbol{\varepsilon}' = \begin{bmatrix} \varepsilon_1 + \varepsilon_2 & 0 & 0 \\ 0 & \varepsilon_1 + \varepsilon_2 & 0 \\ 0 & 0 & \varepsilon_0 \end{bmatrix}. \tag{42}$$

Equation (40) can be written as

$$\mathbf{E}' = \boldsymbol{\varepsilon}'^{-1} \cdot \mathbf{D}', \tag{43}$$

where $\boldsymbol{\varepsilon}'^{-1}$ is the inverse of the dielectric tensor in PCS which can be easily obtained as

$$\boldsymbol{\varepsilon}'^{-1} = \begin{bmatrix} (\varepsilon_1 + \varepsilon_2)^{-1} & 0 & 0 \\ 0 & (\varepsilon_1 - \varepsilon_2)^{-1} & 0 \\ 0 & 0 & \varepsilon_0^{-1} \end{bmatrix}. \tag{44}$$

Consider the wave equation (5) written for the wave propagation of the form (8): i.e.,

$$\frac{\omega^2}{k^2 c^2}\mathbf{D} = \mathbf{E} - \frac{\mathbf{k}(\mathbf{k}\cdot\mathbf{E})}{k^2}. \tag{45}$$

In terms of the direction cosines α_i of the wave vector $\mathbf{k} = (k_\perp, 0, k_\varepsilon)$ one can write Equation (45) as,

$$n^{-2}\mathbf{D} = \mathbf{E} - \boldsymbol{\alpha}(\boldsymbol{\alpha}\cdot\mathbf{E}), \tag{46}$$

where

$$\boldsymbol{\alpha} = (\sin\theta, 0, \cos\theta) \tag{47}$$

and θ is the angle made by the wave vector with $\mathbf{B}_0$.

In the PCS, Equation (46) becomes

$$n^{-2}\mathbf{D}' = \mathbf{E}' - \boldsymbol{\alpha}'(\boldsymbol{\alpha}\cdot\mathbf{E}), \tag{48}$$

as $\boldsymbol{\alpha}\cdot\mathbf{E}$ is invariant under the transformation. Using Equation (43), one can write Equation (48) as

$$(\boldsymbol{\varepsilon}'^{-1} - n^{-2}\mathbf{I})\cdot\mathbf{D}' = \boldsymbol{\alpha}'(\boldsymbol{\alpha}\cdot\mathbf{E}), \tag{49}$$

which can be written in components form using Equation (44) as

$$D_1' = \frac{\alpha_1'(\boldsymbol{\alpha}\cdot\mathbf{E})}{(\varepsilon_1 + \varepsilon_2)^{-1} - n^{-2}}, \tag{50}$$

$$D_2' = \frac{\alpha_2'(\boldsymbol{\alpha}\cdot\mathbf{E})}{(\varepsilon_1 + \varepsilon_2)^{-1} - n^{-2}}, \tag{51}$$

and

$$D_3' = \frac{\alpha_3'(\boldsymbol{\alpha}\cdot\mathbf{E})}{\varepsilon_0^{-1} - n^{-2}}. \tag{52}$$

Now Equation (3) can be written as

$$\boldsymbol{\alpha}\cdot\mathbf{D} = \boldsymbol{\alpha}'^{*}\cdot\mathbf{D}' = 0. \tag{53}$$

i.e.,

$$\alpha_1'^{*}D_1' + \alpha_2'^{*}D_2' + \alpha_3'^{*}D_3' = 0, \tag{54}$$

where $*$ indicates the complex conjugate.

Substituting for D_1', D_2' and D_3' from Equations (50)–(52) into Equation (54) one gets

$$\left[\frac{\alpha_1'^{*}\alpha_1}{(\varepsilon_1 + \varepsilon_2)^{-1} - n^{-2}} + \frac{\alpha_2'^{*}\alpha_2'}{(\varepsilon_1 - \varepsilon_2)^{-1} - n^{-2}} + \frac{\alpha_3'^{*}\alpha_3'}{\varepsilon_0^{-1} - n^{-2}}\right]\boldsymbol{\alpha}\cdot\mathbf{E} = 0. \tag{55}$$

Since $\boldsymbol{\alpha} \cdot \mathbf{E} \neq 0$, we get the dispersion relation

$$\frac{\alpha_1'^* \alpha_1'}{(\varepsilon_1 + \varepsilon_2)^{-1} - n^{-2}} + \frac{\alpha_2'^* \alpha_2'}{(\varepsilon_1 - \varepsilon_2)^{-1} - n^{-2}} + \frac{\alpha_3'^* \alpha_3'}{\varepsilon_0^{-1} - n^{-2}} = 0. \tag{56}$$

In the Cartesian system this becomes

$$\frac{\alpha_1^2 + \alpha_2^2}{R^{-1} - n^{-2}} + \frac{\alpha_1^2 + \alpha_2^2}{L^{-1} - n^{-2}} + \frac{2\alpha_3^2}{\varepsilon_0^{-1} - n^{-2}} = 0, \tag{57}$$

where

$$R = \varepsilon_1 + \varepsilon_2 \quad \text{and} \quad L = \varepsilon_1 - \varepsilon_2. \tag{58}$$

Using Equation (47), Equation (57) can be reduced to the form

$$An^4 - Bn^2 + C = 0, \tag{59}$$

where

$$\begin{aligned} A &= \tfrac{1}{2}(R + L) \sin^2\theta + \varepsilon_0 \cos^2\theta, \\ B &= \tfrac{1}{2}(R + L)\varepsilon_0(1 + \cos^2\theta), \\ C &= \varepsilon_0 RL. \end{aligned} \tag{60}$$

Making use of the expressions for R and L from Equation (58), we can rewrite Equation (60) as

$$\Lambda_c + \Lambda_b = 0, \tag{61}$$

where

$$\Lambda_c = (\varepsilon_1 \sin^2\theta + \varepsilon_0 \cos^2\theta)n^4 - \varepsilon_1\varepsilon_0(1 + \cos^2\theta)n^2 + \varepsilon_0(\varepsilon_1^2 - \varepsilon_2^2) \tag{62}$$

and

$$\Lambda_b = \tfrac{1}{2}\varepsilon_b \sin^2\theta\, n^4 - \tfrac{1}{2}\varepsilon_0\varepsilon_b(1 + \cos^2\theta)n^2 + \varepsilon_0\varepsilon_b(\varepsilon_1 - \varepsilon_2) \tag{63}$$

are the contributions to the dispersion relation from the cold plasma and energetic particles, respectively.

4.3. Analysis of the Dispersion Relation

To find the stability of the three component system, we assume that

$$\omega = \omega_r + i\Gamma, \tag{64}$$

where the real part of the frequency ω_r is much larger than the imaginary part – i.e.,

$$|\Gamma/\omega_r| \ll 1. \tag{65}$$

Therefore, one can write Equation (61) as,

$$\begin{aligned} \Lambda_c + \Lambda_b &= \Lambda_c(\mathbf{k}, \omega_r + i\Gamma) + \operatorname{Re} \Lambda_b(\mathbf{k}, \omega_r) + i \operatorname{Im} \Lambda_b(\mathbf{k}, \omega_r) \\ &= \Lambda_c(\mathbf{k}, \omega_r) + i\Gamma \frac{\partial \Lambda_c(\mathbf{k}, \omega_r)}{\partial \omega_r} + \\ &\quad + \operatorname{Re} \Lambda_b(\mathbf{k}, \omega_r) + i \operatorname{Im} \Lambda_b(\mathbf{k}, \omega_r). \end{aligned} \tag{66}$$

Since the density of the energetic particles is much smaller than that of cold magnetospheric plasma (Wu and Freund, 1977) Re Λ_b can be neglected in comparison with $\Lambda_c(\mathbf{k}, \omega_r)$. This is also in conformity with the assumption that the energetic particles do not alter the dielectric properties of the cold plasma. In view of this, Equation (66) can be separated into real and imaginary parts to obtain

$$\Lambda_c(\mathbf{k}, \omega_r) = 0, \tag{67}$$

and

$$\Gamma = -\left[\frac{\partial \Lambda_c}{\partial \omega_r}\right]^{-1} \text{Im } \Lambda_b. \tag{68}$$

Equation (67) describes the normal modes of the cold plasma which are also called the Appleton–Hartree modes (Akhiezer *et al.*, 1976; Stix, 1962). It can be written for the extraordinary mode with frequency ω_r as

$$n_r^2 = \frac{(\omega_r - \omega_u^c)(\omega_r - \omega_l^c)}{(\omega_r - \omega_u^\infty)(\omega_r - \omega_l^\infty)}, \tag{70}$$

where

$$n_r^2 = k^2/c^2/\omega_r^2,$$

$$\omega_{u,l}^c = \frac{\omega_c}{2}[1 \pm \sqrt{1 + 4\omega_{pc}^2/\omega_c^2}]$$

are the upper and lower cut off frequencies, and

$$\omega_{u,l}^\infty = \frac{\omega_c}{2}[1 \pm \sqrt{1 + 2(\omega_{pc}^2/\omega_c^2)\sin^2\theta}]$$

are the resonance frequencies.

A detailed analysis of Equation (69) gives the propagation characteristics of the X-mode, such as the angular range of propagation where the wave escapes (Ginzburg, 1970; Wu and Freund, 1984; Le Queau *et al.*, 1984). Here we assume that the angle of propagation is such that the radiation in the X-mode reaches the observer when it is amplified by the synchrotron maser mechanism.

Since $\omega_{pc} \ll \omega_c$ in the case of Jovian magnetosphere, we notice that

$$\varepsilon_1 - \varepsilon_2 \simeq 1 - \eta \tag{70}$$

and

$$\varepsilon_0 \simeq 1 - \eta, \tag{71}$$

where

$$\eta = \omega_{pc}^2/\omega_c^2. \tag{72}$$

For the magnetospheric plasma within the Io orbit, it is found that the parameter η varies from about 10^{-1} to 10^{-5} (Wu and Freund, 1977). Moreover, phase velocity of the fast X-mode exceeds the velocity of light. Hence, we can approximate Λ_b as

$$\Lambda_b \simeq \varepsilon_b, \tag{73}$$

where we have neglected terms of order η and k^2c^2/ω_c^2. The task now is to evaluate the integral in ε_b. Substituting for ε_b from Equation (26), making the transformation

to the velocity space using Equation (14) and noting that the Jacobian of transformation is $m^2\gamma^5$, we can rewrite Equation (73) as

$$\Lambda_b = \sum_\alpha \frac{\omega_{p\alpha}^2}{2\omega^2} \int_0^\infty 2\pi v_\perp \, dv_\perp \int_{-\infty}^\infty dv_\parallel \frac{(\omega - k_\parallel v_\parallel) \dfrac{\partial f_{0\alpha}(\mathbf{v})}{\partial v_\perp} + k_\parallel v_\perp \dfrac{\partial f_{0\alpha}(\mathbf{v})}{\partial v_\parallel}}{(\omega - k_\parallel v_\parallel - \omega_c \gamma^{-1})}. \tag{74}$$

As already stated, we use the loss cone distribution for the energetic electrons: i.e.,

$$f_{0\alpha}(\mathbf{v}) = \frac{1}{\pi^{3/2} v_{t\alpha}^3 q!} \left(\frac{v_\perp}{v_{t\alpha}}\right)^{2q} \exp\left[-\frac{v_\perp^2 + (v_\parallel - u)^2}{v_{t\alpha}^2}\right], \tag{75}$$

where we have assumed isotropic temperature $T_\alpha = m v_{t\alpha}^2$. Substituting Equation (75) into Equation (74), one can perform the integration in two ways: either one can use the Plemelj formula (e.g., Wu and Freund, 1984), or follow the expansion method given by Le Queau *et al.* (1984). Following the latter method, we can write Equation (74) as,

$$\Lambda_b = \sum_\alpha \Lambda_b^\alpha \tag{76}$$

where

$$\Lambda_b^\alpha = -i \frac{2\omega_{p\alpha}^2 c^2}{\omega^2 v_{t\alpha}^2} \left[q I_{q+1}^\alpha - (q+1) I_{q+2}^\alpha - \right.$$
$$\left. - \frac{v_{t\alpha}^2}{c^2} A_\alpha (q+1) \left(A_\alpha + \frac{u_\alpha}{v_{t\alpha}}\right) (I_{q+2}^\alpha - I_{q+3}^\alpha) \right] \tag{77}$$

with

$$I_q^\alpha = \int_1^{1-i\infty} dz \, (z)^{-q-1/2} \exp\left[A_\alpha^2 z^{-1} + B_\alpha^2 z - A_\alpha^2 - B_\alpha^2\right], \tag{78}$$

where we have defined

$$A_\alpha = \frac{c}{v_{t\alpha}} \left(\frac{k_\parallel c}{\omega_c} - \frac{u_\alpha}{c}\right) \tag{79}$$

and

$$B_\alpha = \frac{c}{v_{t\alpha}} \left(\frac{k_\parallel^2 c^2}{\omega_c^2} - \frac{2(\omega_r - \omega_c)}{\omega_c}\right)^{1/2}. \tag{80}$$

The integrals I_q satisfy the recurrence relation

$$A^2 I_{q+1} = 1 - (n - \tfrac{1}{2}) I_q + B^2 I_{q-1}. \tag{81}$$

Evaluation of the integrals give (Le Queau *et al.*, 1984)

$$\mathrm{Im}\,(I_{q+1}^\alpha) = -\sqrt{\pi} (2B_\alpha)^{2q+1} \exp(-A_\alpha^2 - B_\alpha^2) \sum_{p=0}^\infty \frac{(p+q)! (2A_\alpha B_\alpha)^{2p}}{p! [2(p+q)+1]!}. \tag{82}$$

It is clear from Equation (82) that the imaginary part of I_{q+1} is large for $A_\alpha \to 0$ or $A_\alpha \to \infty$. Actually, for large values of A_α and B_α, the instability is the relativistic

counterpart of the Weibel instability (Melrose, 1979). For small values of A_α and B_α, the instability is synchrotron maser instability (SMI) which has no non-relativistic counterpart. Since we are interested in SMI, we assume that $A_\alpha \ll 1$ and hence we will keep only the lowest order terms in Equation (83). Substitution of Equation (82) into Equation (68) gives the growth rate of the SMI in the presence of the energetic particles. It is obvious from Equation (68) that the maser acts when Im $\Lambda_b < 0$. In what follows we will discuss the growth rate in the context of Jovian shadow events.

5. Application to Jovian Shadow Events

5.1. SMI GROWTH RATE IN THE PRESENCE OF S-ELECTRONS

The bunch of electrons causing the L-emission has loss cone distribution. For simplicity, we take $q = 1$ in Equation (75) for L-electrons – i.e.,

$$f_{0\mathrm{L}} = \frac{1}{\pi^{3/2} v_{t\mathrm{L}}^3} \left(\frac{v_\perp}{v_{t\mathrm{L}}}\right)^2 \exp\left[-\frac{v_\parallel - (v_\parallel - U_\mathrm{L})^2}{v_{t\mathrm{L}}^2}\right]. \tag{83}$$

For the S-electrons, we assume a shifted Maxwellian which could be obtained from Equation (75) setting $q = 0$ – i.e.,

$$f_{0\mathrm{S}} = \frac{1}{\pi^{3/2} v_{t\mathrm{S}}^3} \exp\left[-\frac{v_\parallel + (v_\parallel - U_\mathrm{S})^2}{v_{t\mathrm{S}}^2}\right]. \tag{84}$$

Note that the S-electron bunch does not contribute to the maser type of instability because the distribution given by Equation (84) does not have a population inversion. Under the small A_α assumption Equation (77) becomes

$$\Lambda_b^{\mathrm{L}} = -\frac{2\omega_{p\mathrm{L}}^2}{\omega_r^2} \frac{c^2}{v_{t\mathrm{L}}^2} \frac{8\sqrt{\pi}}{3} B_\mathrm{L}^3 \exp(-B_\mathrm{L}^2)\left[1 - \tfrac{4}{5} B_\mathrm{L}^2 \left(1 + \frac{v_{t\mathrm{L}}^2}{c^2} \frac{U_\mathrm{L}}{v_{t\mathrm{L}}} A_\mathrm{L}\right)\right], \tag{85}$$

and

$$\Lambda_b^{\mathrm{S}} = \frac{\omega_{p\mathrm{S}}^2}{\omega_r^2} \frac{c^2}{v_{t\mathrm{S}}^2} \frac{8\sqrt{\pi}}{3} B_\mathrm{S}^3 \exp(-B_\mathrm{S}^2)\left[1 + \frac{v_{t\mathrm{S}}^2}{c^2} \frac{U_\mathrm{S}}{v_{t\mathrm{S}}} A_\mathrm{S}\right], \tag{86}$$

where Λ_b^α now represents the imaginary part of Λ_b^α. The growth rate (68) can now be written as

$$\begin{aligned}\Gamma &= -\left[\frac{\partial \Lambda_c}{\partial \omega_r}\right]^{-1} \Lambda_b^{\mathrm{L}} \left(1 + \frac{\Lambda_b^{\mathrm{S}}}{\Lambda_b^{\mathrm{L}}}\right) \\ &= -\left[\frac{\partial \Lambda_c}{\partial \omega_r}\right]^{-1} \Lambda_b^{\mathrm{L}} \left\{1 - \frac{N_\mathrm{S}}{N_\mathrm{L}} \left(\frac{T_\mathrm{L}}{T_\mathrm{S}}\right)^{5/2} \exp\left[-B_\mathrm{L}^2 \left(\frac{T_\mathrm{L}}{T_\mathrm{S}} - 1\right)\right] \times \right. \\ &\quad \left. \times \frac{1 + \frac{U_\mathrm{S}}{c}\left(\frac{k_\parallel c}{\omega_c} - \frac{U_\mathrm{S}}{c}\right)}{1 + \frac{4}{5} B_\mathrm{L}^2 \left[1 + \frac{U_\mathrm{L}}{c}\left(\frac{k_\parallel c}{\omega_c} - \frac{U_\mathrm{L}}{c}\right)\right]} \right\},\end{aligned} \tag{87}$$

where we have written $\omega_{p\alpha}$ and $v_{t\alpha}$ in terms of density N_α and temperature T_α and used the expression (79) for A_α. Equation (87) indicates that when the S-electrons are absent ($N_S = 0$), the growth rate reduces to that of the usual SMI for a loss cone distribution of L-electrons: i.e.,

$$\begin{aligned}\Gamma_0 &= -\left[\frac{\partial \Lambda_c}{\partial \omega_r}\right]^{-1} \Lambda_b^L \\ &= \left[\frac{\partial \Lambda_c}{\partial \omega_r}\right]^{-1} \frac{8\sqrt{\pi}}{3} \frac{\omega_{pL}^2}{\omega_r^2} \frac{c^2}{v_{tL}^2} B_L^3 \exp(-B_L^2) \times \\ &\quad \times \left\{1 - \tfrac{4}{5} B_L^2 \left[1 + \frac{U_L}{c}\left(\frac{k_\parallel c}{\omega_c} - \frac{U_L}{c}\right)\right]\right\}. \end{aligned} \tag{88}$$

This growth rate has been extensively studied under various circumstances for both Jovian decametric emission and auroral kilometric radiation (Freund and Wu, 1977; Le Queau *et al.*, 1984; Pritchell, 1984). When $\Gamma_0 > 0$, the SMI acts and the L-emission occurs.

According to Equation (88), the SMI grows when

$$B_L^2 \lesssim \tfrac{5}{4}, \tag{89}$$

since

$$\frac{U_L}{c}\left(\frac{k_\parallel c}{\omega_c} - \frac{U_L}{c}\right) \ll 1$$

for a weakly relativistic plasma. When the L-emission is in progress, the inequality (89) is satisfied.

It is clear from Equation (87) that the presence of S-electrons reduces the growth rate of the SMI and the reduction depends upon the density, temperature and very weakly on the velocity of the S-electrons. Neglecting the corrections from the terms proportional to U_L/c, U_S/c, we find some interesting special cases of Equation (88):

(1) for $B_L = 0$,

$$\frac{\Gamma}{\Gamma_0} = 1 - \left(\frac{N_S}{N_L}\right)\left(\frac{T_L}{T_S}\right)^{5/2}, \tag{90}$$

which shows that the instability is completely quenched when

$$\left(\frac{N_S}{N_L}\right) = \left(\frac{T_S}{T_L}\right)^{5/2}, \tag{91}$$

(2) for $T_L = T_S$,

$$\frac{\Gamma}{\Gamma_0} = 1 - \left(\frac{N_S}{N_L}\right)(1 - \tfrac{4}{5}B_L^2)^{-1} \tag{92}$$

in which case the instability disappears for

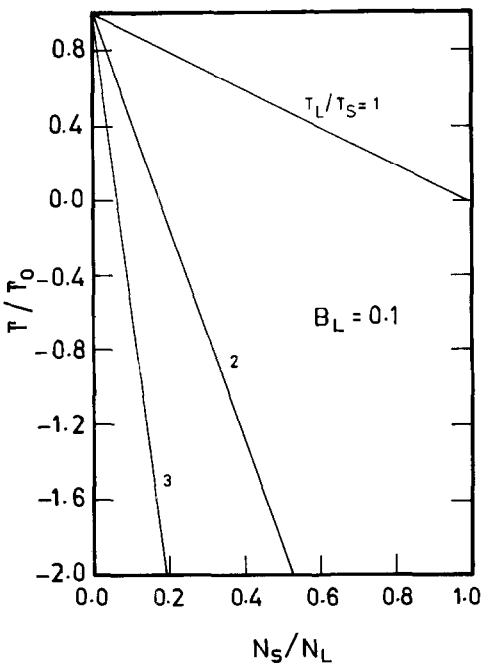

Fig. 1. The behaviour of the normalized growth rate Γ/Γ_0 as a function of the density ratio N_S/N_L, for fixed value of B_L.

$$\frac{N_S}{N_L} = 1 - \tfrac{4}{5}B_L^2. \tag{93}$$

The growth rate Γ/Γ_0 is plotted for various values of the parameters N_S/N_L, T_L/T_S and B_L in Figures 1–5. Figures 1 and 2 give the variation of the growth rate with respect to the density ratio. They are the curves given by Equations (91) and (92), respectively. Figure 3 shows that even for a very small density ratio, the growth rate is drastically reduced for $T_L/T_S < 3$. For $T_L/T_S > 3$, the growth rate Γ again increases but never reaches Γ_0. When the value of density is slightly increased, the fall of growth rate is still drastic and the instability is completely quenched even for T_L/T_S less than unity. Figure 4 is the same as Figure 1 but the variation of growth rate with respect to the parameter B_L is given. Figure 5 is the same as Figure 3 but for higher density ratio and indicates again the rapid fall of the growth rate.

It is clear from the above discussions that the invasion of S-electrons into the L-emission region quenches the SMI, thereby stopping the L-emission. Physically speaking, when the S-electrons coexist with the L-electrons, the combined distribution ceases to be a loss cone distribution. The loss cone is partially or completely filled by the S-electrons, the population inversion is destroyed and hence the instability is quenched as the free energy source is cut off. Once the S-electrons leave the L-emission

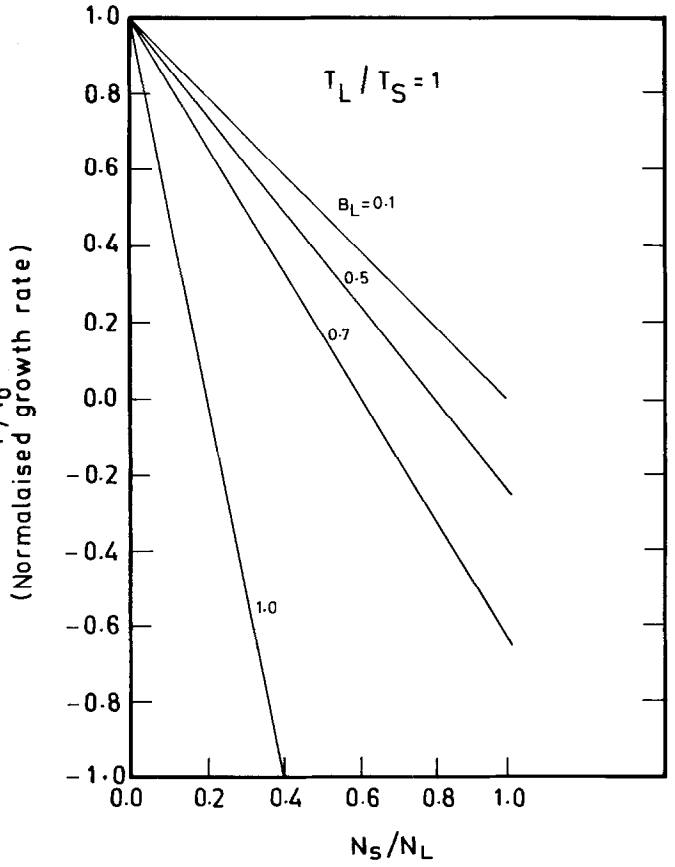

Fig. 2. Same as Figure 1 for $T_L = T_S$.

region, the L-emission is gained as the loss cone is re-established. Such a loss conefilling mechanism has been used in the context of sudden reductions in solar decimetric continuum by Benz and Kuijpers (1976) where the quenching of electrostatic loss cone instabilities were considered. The typical value of $\omega_{pc}^2/\omega_c^2 \sim 10^{-3}$ for the Jovian magnetosphere within about 6 Jovian radii (Wu and Freund, 1977) and for L-electron temperatures if one assumes $v_{tL}/c \sim 10^{-1}$, then the growth rate in the absence of S-electrons is 10^6; so, the growth time is in the micro second range. The single frequency duration of the shadow events roughly gives the duration of S–L interaction at a particular layer. As this duration is of the order of milliseconds, the S-beams coexist with the L-electrons for thousands of growth times of the SMI and hence the emission will be cut off. In what follows we consider the specific observed features of the shadow events and explain them using the present theory.

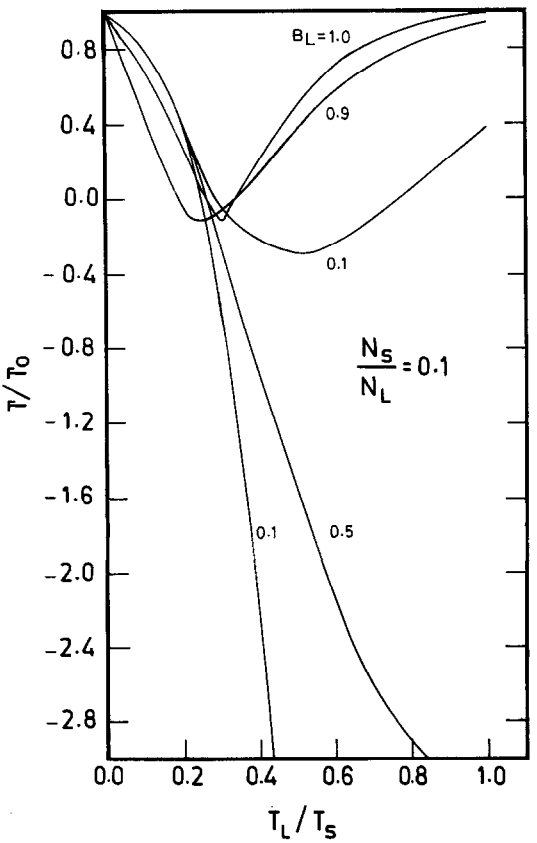

Fig. 3. The behaviour of the normalised growth rate Γ/Γ_0 as a function of the temperature ratio T_L/T_S, for $N_S/N_L = 0.1$.

5.2. Interpretation of Observed Features

As already mentioned, S-bursts occur in pairs originating from a vertex. Near the vertex, the region in between the bursts also shows emission (Leblanc *et al.*, 1980). If the S-emission is due to bunches of electrons, then, there must be an electron population in between the bunches near the vertex to give observable emission. As the S-electron bunches move along the Io flux tube (IFT), the separation between them increases. The middle electron population (MEP) in between the bunches spreads into this increased region, thus becoming less dense. As the synchrotron emissivity depends upon the electron density, the MEP away from the vertex ceases to produce observable S-emission, but still has considerable density. These 'invisible' electrons while passing through the L-emission region fill the loss cone of L-electrons and quench the instability. The pair of S-bursts, therefore, appears to be aligned along the edges of the emission gap produced by the MEP. The V-shape of the shadow event

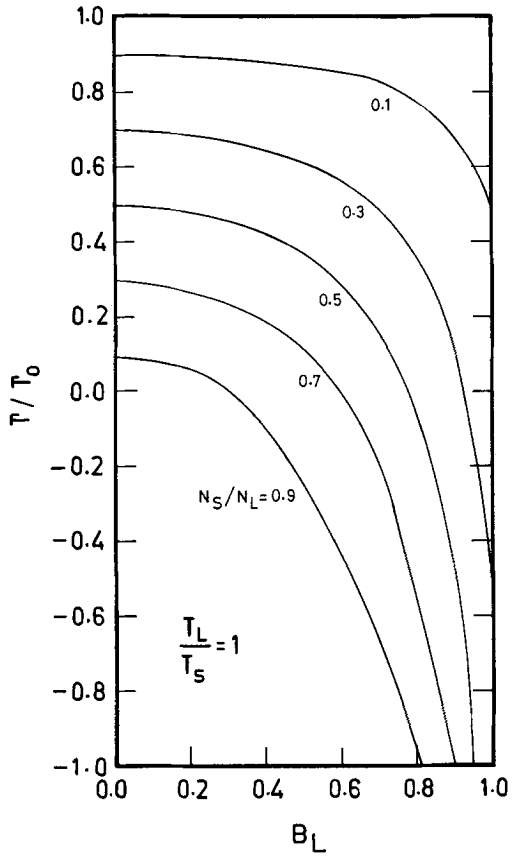

Fig. 4. The behaviour of the normalised growth rate as a function of the parameter B_L for various density ratios in the equal temperature case.

is therefore accounted for as the MEP always fills the region between the pair of S-electron bunches.

The cases where only one of the S-bursts is aligned along one edge of the shadow can be traced back to the origin of the S-electron buynches. Staelin and Rosenkranz (1983) have proposed a modulation hypothesis where electron beams injected into the IFT are supposed to be modulated by very low frequency waves near Jovian ionosphere. As in the case of klystron, electron bunching takes place and within a short distance, depending upon the amplitude and frequency of modulation, the bunch bifurcates forming a pair of leading and a trailing bunches. It is possible that the modulating electric fields can have such characteristics as to produce pairs of bunches where one of them could be less dense and may not radiate for a long time throughout their journey from the vertex. If this bunch also becomes invisible like the MEP, then a shadow event is produced where only one burst is aligned alone one edge

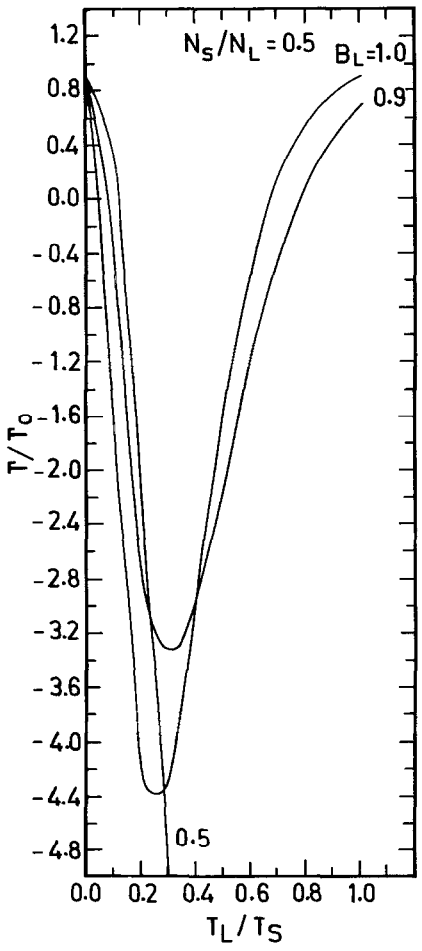

Fig. 5. Same as Figure 3. For $N_S/N_L = 0.5$.

of the emission gap. The complex type of shadow patterns obtained in certain cases (e.g., Riihimaa, 1981) may be due to a complex wave form of the modulating field and aperiodic modulations.

The single streaks of shadow events at high frequencies correspond to the stages prior to the formation of vertex. Since these are close to the injection regions, the electron beams are less dense and start bunching to form the vertex. The electrons prior to the vertex formation could again be 'invisible' and if they invade an L-emission region, they could produce single streaks of shadow events. This is supported by the fact that single streaks are observed only at high frequencies. Another related effect is the S-emission which appear to grow out of shadow events at high frequencies. In this case the electrons in the pre-bunching stage pass through L-emission

region and after crossing, the bunching takes place to sufficiently high density to produce observable emission and thus they appear to grow out of the shadow streaks.

The single frequency duration could be interpreted as the time taken by the MEP to cross a particular layer of emission. At high frequencies, the separation between the two S-bunches in a pair is quite small and hence the extent of MEP is small. The transit time of the MEP, therefore, is small and hence one observes that the shadow bursts have smaller duration at high frequencies. At low frequencies, the bunches are far away from the vertex and their separation increases considerably. The separation between the bunches is the same as the extent of MEP and naturally one expects longer duration at low frequencies.

The observation that shadow events are more abundant at high frequencies naturally follows from the fact that S-electrons are injected from the planet. As all the beams need not be of the same concentration, many of the beams need not pass all through the IFT. Some of the beams may not reach the regions of minimum magnetic field, and hence there are less shadow events at low frequencies.

6. Discussion and Conclusions

We have discussed that S-electrons which do not produce observable synchrotron radiation (invisible) can cause the shadow events. The electrons have to be invisible because, otherwise the S-emission will 'light up' the shadow. Of course, one has to compare the detection limit of a particular radio telescope with the theoretical value of the flux of gyrosynchrotron radiation of S-electrons to estimate the density at which they become invisible. The instability can be quenched by S-electrons with a small density, an order of magnitude less than that of the L-electrons.

Though we have assumed a shifted Maxwellian distribution for the invading electrons, the correct distribution has to be determined from the modulation wave form. The result will not change so long as the invading electrons fill the loss cone of the L-emitting bunch and by themselves do not have a population inversion. We have not taken into account the curvature and inhomogeneity of the Jovian magnetic field. This is justified because of the smallness of the L-emission regions (as evident from the small bandwidth) compared to the scale lengths of inhomogeneity. The theory accounts for most of the observed features. It could be made more quantitative if the modulation hypothesis could be well established, for example, by identifying the type of low frequency waves responsible for modulation and if the electron acceleration mechanism is unambiguously identified. This is a task for the future.

Acknowledgement

The author is thankful for the helpful discussions with Dr. Ch. V. Sastry.

References

Akhiezer, A. L., Akhiezer, I. A., Polovin, R. V., Sitenko, A. G., and Stepanov, K. N.: 1967, in *Collective Oscillations in a Plasma*, Pergamon Press, Oxford.

Baldwin, E. D., Bernstein, I-B., and Weenik, M. P. H.: 1969, in *Advances in Plasma Physics*, Vol. 3, John Wiley, New York.

Benz, A. O. and Kuijpers, J.: 1976, *Solar Phys.* **46**, 275.

Desch, M. D., Flagg, R. S., and May, J.: 1978, *Nature* **272**, 38.

Ellis, G. R. A.: 1973, *Nature* **241**, 387.

Flagg, R. S., Krausche, D. S., and Lebo, G. R.: 1976, *Icarus* **29**, 477.

Galeev, A. A. and Krasnoselskikh, V. V.: 1979, *Sov. Astron. Lett.* **5**, 257.

Ginzburg, V. L.: 1970, *The Propagation of Electromagnetic Waves in Plasmas*, Pergamon Press.

Gordon, M. A.: 1966, Ph.D. Thesis, University of Colorado.

Groth, M. J. and Dowden, R. L.: 1975, *Nature* **255**, 382.

Gurnett, D. A. and Goertz, C. K.: 1981, *J. Geophys. Res.* **86**, 717.

Hewitt, R. G., Melrose, D. B., and Ronnmark, K. G.: 1982, *Aust. J. Phys.* **35**, 447.

Hirshfild, J. L. and Bekefi, G.: 1963, *Nature* **198**, 20.

Krausche, D. S., Flagg, R. S., Lebo, G. R., and Smith, A. G.: 1976, *Icarus* **29**, 463.

Leblanc, Y., Aubier, M. G., Rosolen, C., Genova, F., and de la Noe, J.: 1980, *Astron. Astrophys.* **86**, 349.

Le Queau, D., Pellat, R., and Roux, A.: 1984, *Phys. Fluids* **27**, 247.

Melrose, D. B.: 1979, *Astrophys. J.* **230**, 621.

Melrose, D. B.: 1982, in A. O. Benz and P. Zlobec (eds.), *Proceedings of the 4th CESRA Workshop on Solar Noise Storms*, Trieste, p. 182.

Pritchett, P. L.: 1984, *J. Geophys. Res.* **89**, 8957.

Riihimaa, J. J. and Warwick, J. W.: 1968, *Astrophys. Lett.* **2**, 185.

Riihimaa, J. J., Carr, T. D., Flagg, R. S., Greenman, W. B., Gombola, P. P., Lebo, G. R., and Levy, J. A.: 1981, *Icarus* **48**, 298.

Sharma, R. A., Vlahos, L., and Papadopoulos, K.: 1982, *Astron. Astrophys.* **112**, 377.

Smith, R. A.: 1976, in T. Gehrels (ed.), *Jupiter, the Giant Planet*, University of Arizone Press, Tucson.

Staelin, D. H. and Rosenkranz, P. W.: 1983, M.L.T. Preprint.

Stix, T.: 1962, *The Theory of Plasma Waves*, McGraw-Hill, New York.

Wu, C. S. and Freund, H. P.: 1977, *Astrophys. J.* **213**, 575.

Wu, C. S. and Freund, H. P.: 1984, *Radio Science* **19**, 519.